Chemical Research in Toxicology

pubs.acs.org/crt

Article

Identification of a Noncanonical Necrotic Cell Death Triggered via Enhanced Proteolysis by a Novel Sapogenol Derivative

Göklem Üner, Özgür Tağ, Yalçın Erzurumlu, Petek Ballar Kirmizibayrak,* and Erdal Bedir*

Cite This: *Chem. Res. Toxicol.* 2020, 33, 2880−2891

Read Online

ACCESS | Metrics & More | Article Recommendations | Supporting Information

ABSTRACT: Small molecules which activate distinct cell death pathways have promising high potential for anticancer drug research. Especially, regulated necrosis draws attention as an alternative cell death mechanism to overcome the drug resistance. Here, we report that a new semisynthetic saponin analogue (AG-08) triggers necrotic cell death with unprecedented pathways. AG-08-mediated necrosis depends on enhanced global proteolysis involving calpains, cathepsins, and caspases. Moreover, AG-08 generates several alterations in lysosomal function and physiology including membrane permeabilization, redistribution toward the perinuclear area, and lastly excessive tubulation. As a consequence of lysosomal impairment, the autophagic process was abolished via AG-08 treatment. Collectively, in addition to its ability to induce necrotic cell death, which makes AG-08 a promising candidate to cope with drug resistance, its unique activity mechanisms including autophagy/lysosome impairment and enhancement of proteolysis leading a strong death capacity emphasizes its potential for anticancer drug research.

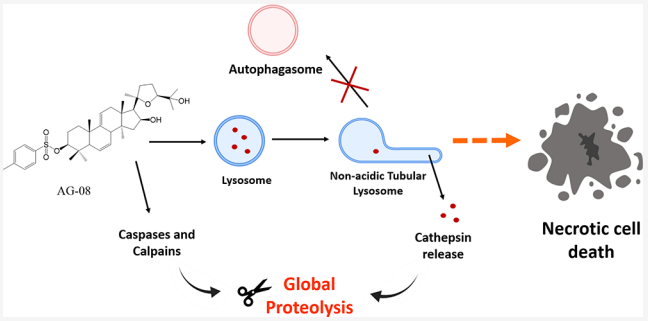

INTRODUCTION

Saponins are secondary metabolites possessing sugar units on triterpenoid or steroidal skeletons. They have broad biological activities, including antimicrobial, anti-inflammatory, and antitumor.[1] Since the antitumor potency of saponins is in general relatively weak, scientists have begun bioassay-directed drug design and synthesis studies anticipating highly potent novel structures. One of these studies has revealed that a semisynthetic oleanane-type saponin, viz., 2-cyano-3,12-dioxoolean-1,9-dien-28-oic acid methyl ester (CDDO-Me), is a multifunctional molecule with promising clinical potential as a chemopreventive and chemotherapeutic agent. Compared to its starting molecule, CDDO-Me inhibited nitric oxide generation up to 10 000-fold verifying that semisynthesis is an auspicious approach to develop potent saponin-based drugs.[2] Currently, semisynthetic anticancer drug-discovery programs have mainly engaged with commercially available natural products. Indeed, oleanolic acid, ursolic acid, and betulinic acid are widely studied triterpenoids compared to the less common miscellaneous aglycons such as cycloartanes.

Development of drug resistance is one of the major problems in anticancer therapy since most of the unsuccessful chemotherapy treatments are related to drug resistance.[3] One leading reason for anticancer drug resistance is that most chemotherapeutics invoke apoptosis while many cancer cells, especially metastatic cells, develop resistance to apoptotic mechanisms. Therefore, the induction of nonapoptotic cell death pathways becomes a strategy to increase the success of cancer treatments.[4,5] In this regard, compounds that trigger necrosis arise as novel anticancer drug candidates. Subsequently, intensely performed studies indicate that certain types of necrosis can also be regulated by complex cellular signaling mechanisms and therefore are proposed as new targetable pathways in cancer treatment.[6−10]

In a project aiming to prepare new antitumor agents from cycloartane-type sapogenins, we discovered a cytotoxic analogue (AG-08) which induced a noncanonical necrotic cell death depending on augmented global proteolysis. Main cellular proteases including calpains, cathepsins, and interestingly caspase 3, 7 and 8, widely known as apoptosis inducers, were activated via AG-08 treatment. Besides the activation of several proteases, lysosomal membrane permeabilization, lysosomal redistribution toward the perinuclear area, and excessive lysosomal tubulation were observed with AG-08 treatment. Furthermore, AG-08 inhibited autophagy flux due to the lysosomal impairment. Concomitant to the enhancement of proteases, a high concentration of AG-08 also contributed to the inhibition of autophagy via the cleavage of Atg proteins.

Received: August 13, 2020
Published: November 2, 2020

Downloaded via IZMIR YUKSEK TEKNOLOJI ENSTITUSU on November 22, 2022 at 07:34:25 (UTC).
See https://pubs.acs.org/sharingguidelines for options on how to legitimately share published articles.

© 2020 American Chemical Society

https://dx.doi.org/10.1021/acs.chemrestox.0c00339
Chem. Res. Toxicol. 2020, 33, 2880−2891

Our results indicate that AG-08 possesses a great potential for anticancer drug discovery research by triggering non-canonical necrosis along with increased global proteolysis, impairment of lysosomal activity, and inhibition of autophagy since molecules that induce alternative cell death pathways rather than apoptosis have been stated as promising in overcoming drug resistance.

MATERIALS AND METHODS

Semisynthesis of AG-08. Cycloastragenol (CG) was donated by Bionorm Natural Products Production & Marketing Co., İzmir, Turkey. Twenty grams of CG was dissolved with 400 mL of methanol, and 10 mL of concentrated sulfuric acid was added to this solution. Reaction was continued for 6 h at reflux. Then reaction mixture was neutralized with NaOH and dried with an evaporator at 60 °C. First, acetonitrile precipitation and then a silica gel RP-18 (Fluka) column with 60:40 acetone:water was used for purified AG (60.6% yield). To synthesize the AG-08, 1 g of AG was dissolved in 12 mL of pyridine, and 1.8 g of *p*-TsCl (*p*-tosyl chloride, Acros Organics) reagent was added. Reaction was continued for 4 h at room temperature. Then the reaction mixture was quenched by the addition of 100 mL of distilled water. Following the extraction via 200 mL of ethyl acetate (three times), the extract was evaporated at 60 °C in the rotary evaporator. Lastly, AG-08 was purified from the dried reaction mixture on silica gel (Kiesegel 60, 70-230 mesh, Sigma-Aldrich) which was conditioned by 8:2 hexane:EtOAc (34.7% yield).

Chemicals. Cathepsin inhibitor I (Calbiochem, 219415) as cathepsin B, L, S inhibitor, Z-VAD-fmk (Enzo; ALX-26-020-M001) as pan-caspase inhibitor, and Z-IETD-fmk (Abcam; ab141382) as caspase 8 inhibitor were used in protease inhibition studies. Staurosporine (9953) and bafilomycin A1 (54645) were purchased from Cell signaling. Cycloheximide (66-81-9) was purchased from Calbiochem.

Cell Culture. HCC1937 (human breast cancer line), HeLa (human endometrial carcinoma), A549 (human lung adenocarcinoma), IMR-90 (human lung fibroblasts), C2C12 (mouse myoblast cells), Vero (Cercopithecus aethiops kidney cell line), LNCaP (prostate adenocarcinoma), MRC-5 (human lung fibroblasts), MCF7 (human breast cancer cells), DU145 (human prostate adenocarcinoma), and H295R (human adrenocarcinoma) were obtained from American Type Culture Collection and maintained as exponentially growing monolayers by culturing according to the supplier's instructions. C2C12, Vero, IMR-90, MCF7, HeLa, MRC-5, and DU145 cell lines were cultured and routinely passaged in DMEM media containing 10% FBS, while LNCaP and HCC1937 cell lines were propagated in RPMI 1640 containing 10% FBS. H295R cells were cultured in DMEM/F12 media containing 10% FBS.

Cytotoxicity Analysis. Following the treatment with AG-08 or vehicle for 48 h, the 10% WST-1 (Roche, Switzerland) in the medium was replaced in each 96-well. After 4 h incubation with WST-1 reagent at 37 °C and 5% CO_2, absorbance was measured by using a microplate reader at 440 nm (Varioscan, Thermo Fisher Scientific, USA). Graph Pad Prism 5 (San Diego, CA) was used to calculate the IC_{50}, which represents the concentration of compound that is required for 50% inhibition in comparison to the vehicle-treated controls. The experiments were repeated three times independently.

Western Blot Analysis. Cell lysates were prepared by RIPA buffer (1XPBS, 1% nonidet P-40, 0.5% sodium deoxycholate, and 0.1% SDS, pH 8.0). Protein concentrations were determined by bicinchoninic acid (BCA) protein assay (Thermo Fisher Scientific, USA). After equal amounts of proteins were loaded to the gels, proteins were separated by SDS-PAGE electrophoresis and transferred to PVDF membranes (EMD Millipore, Thermo Fisher Scientific, USA). Following the classic immunoblotting steps (blocking, incubating with primary and secondary antibodies), chemiluminescence signals were detected using Clarity ECL substrate solution (Bio-Rad, US) by Fusion-FX7 (Vilber Lourmat, Thermo Fisher Scientific, USA). Monoclonal antibodies used in this study were anticaspase-9 (CST-9508, USA), anticaspase-8 (CST-9746, USA), anti-LC3 (CST-12741, USA), anti-Atg-3 (CST-3415, USA), anti-Atg-9a (CST-13509, U.K.), anti-Atg-5/12 (CST-12994, USA), anti-Atg-7 (CST-8558, USA), anti-Atg-16L1 (CST-8089, U.K.), antiactin (Sigma-Aldrich-A5316, U.K.), anticaspase-3 (CST-9665, USA), anti-PARP-1 (CST-9542, USA), anti-CHOP (CST-2895, U.K.), anti-K48-linkage specific polyubiquitin (CST-12805), and anti-p62 (Proteintech-184201AP, USA). The experiments were repeated three times independently, with one representative result shown.

Total RNA Isolation and Expression Analysis by Quantitative RT-PCR. The total RNA was isolated using a Total RNA Isolation Kit (Bio-Rad, USA) following the manufacturer's instructions. cDNAs were synthesized using the iScript cDNA synthesis kit (Bio-Rad, USA) according to the manufacturer's instructions. For gene expression analysis, specific primers were designed against p62, Atg-3, Atg-5, and CHOP (Supporting Information Table 3). Quantitative RT-PCR (qRT-PCR) was performed using the SYBR Green I Mastermix (Bio-Rad, USA) and LightCycler480 thermocycler (Roche). Fold changes for the transcripts were normalized to the housekeeping gene TBP1 (TATA-Box Binding Protein1). The reaction efficiency incorporated ΔΔCq formula was used for relative quantification. Six independent biological replicates with two technical replicates per experiment were used for each PCR.

Lysosome Staining. Cells were seeded on the coverslips and treated with AG-08. Then the cells were incubated with 50 nM LysoTracker Red DND-99 in prewarmed fresh medium for 40 min at 37 °C and 5% CO_2. After mounting, cells were immediately observed using a fluorescence microscope (Olympus IX70).

LDH (Lactate Dehydrogenase) Releasing Assay. A LDH-Cytotoxicity Colorimetric Assay Kit II (Biovision) was used to detect the LDH release. Briefly, HCC1937 was seeded on a 96-well plate. After treatment with AG-08, the cells were centrifuged at 600 *g* for 10 min. Ten microliters of supernatant was transferred into clean 96-well plates, and 100 μL of LDH Reaction Mix was added. Following 30 min incubation at room temperature, 10 μL of stop solution was added, and the absorbance was measured at 450 nm (Varioscan, Thermo Fisher Scientific, USA).

Immunofluorescence Studies. Cells were grown on glass coverslips and treated with AG-08. At the end of the treatments, the cells were washed twice with ice cold PBS and fixed with 4% paraformaldehyde in PBS for 30 min at 4 °C. After being washed six times with PBS, the cells were permeabilized and blocked with 0.01% saponin and 0.01% BSA in PBS. Then the fixed cells were incubated with primary antibodies for 1 h at 37 °C. LAMP1 (CST-9091, USA) antibody was used at 1:200 dilutions. Cells were then

https://dx.doi.org/10.1021/acs.chemrestox.0c00339
Chem. Res. Toxicol. 2020, 33, 2880−2891

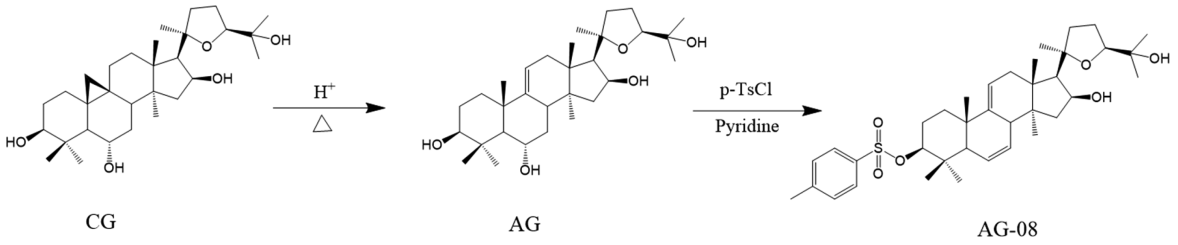

Figure 1. Schematic illustration of the semisynthesis of AG-08 from CG.

incubated with secondary antibodies (1:400) for 1 h at 37 °C. Mounted samples were analyzed by fluorescence microscopy (Olympus IX70, Japan).

Subcellular Fractionation and Cathepsin Activity. After treatment with AG-08 and vehicle, cells were harvested and resuspended in fractionation buffer (50 mM TrisHCl, 0.32 M sucrose, 10 mM TEA (triethaanolamine), 1 mM EDTA, 1 mM 2-mercaptoethanol, pH = 8). Then the cells were incubated 10 min on ice and passed 20 times through a gauge. After the first centrifugation at 1000 *g* for 5 min (three times), the supernatant was centrifuged again at 51 000 rpm for 1 h, and the supernatant was saved as a cytoplasmic fraction. To determine the cathepsin B/L/S activity, the cytoplasmic fraction was incubated with 30 μM fluorogenic substrate Z-Phe-Arg-AMC (Z-FR-AMC) and 5 μM DTT in 100 mM phosphate buffer (pH 6.0) for 30 min at 37 °C. After incubation, the fluorescence intensity was measured with a microplate reader (370 nm for excitation and 460 nm for the emission wavelength) (Varioscan, Thermo Fisher Scientific, USA).

Calpain Activity. The calpain activity of the cells was determined using a Calpain Activity Fluorometric Assay Kit (BioVision Inc.) according to the manufacturer's instructions. In brief, the cells were extracted with an extraction buffer supplied by the manufacturer, and then an equal amount of protein lysate was mixed with the fluorescence-labeled substrate for 1 h. Lastly, the fluorescence intensity was measured with a microplate reader (Varioscan, Thermo Fisher Scientific, USA).

Filipin III Staining. Cells were grown on glass coverslips and treated with AG-08 or vehicle. At the end of the treatments, the cells were fixed with 4% paraformaldehyde in PBS for 30 min at 4 °C. After being washed six times with PBS, the cells were permeabilized and blocked with 0.01% saponin and 0.01% BSA in PBS. Then the fixed cells were incubated with 25 μM filipin III (Cayman, 70440) for 1 h at 37 °C. After being washed with PBS two times, the mounted samples were immediately analyzed by fluorescence microscopy (Olympus IX70, Japan).

Proteasomal Activity. After the treatment with AG-08 or vehicle, cells were harvested and resuspended in 0.5 μM DTT containing lysis buffer (8.56 g of saccharose, 0.6 g of HEPES, 0.2 g of $MgCl_2$, 0.037 g of EDTA in 100 mL of H_2O; pH = 7.8). The samples were incubated in the liquid nitrogen for 15 s and subsequently in a 40 °C water bath for 1 min (three cycles). Then lysate was centrifuged at 13 400 rpm for 10 min. Ten microliters of each supernatant was incubated with 10 μL of Suc-Leu-Leu-Val-Tyr AMC and 90 μL of a master mix which involves 0.2 μL of 1 M DTT, 56.5 μL of H_2O, and 33.3 μL of incubation buffer (13.63 g of Tris base, 1.68 g of KCl, 0.8 g of Mg acetate·$4H_2O$, 0.76 g of $MgCl_2$·$6H_2O$ in 250 mL of H_2O; pH = 8.2). Following 1 h incubation at 37 °C, the fluorescence intensity was measured at 360 nm excitation and 460 nm emission wavelengths. To determine the direct effect of AG-08 on the proteasome, nontreated cells were lysed via the described method. Then, the solution containing lysate and master mix was incubated with AG-08 or vehicle for 1 h at 37 °C. Lastly, Suc-Leu-Leu-Val-Tyr AMC was utilized to determine the proteasome activity with the method mentioned above.

Flow Cytometry. Cell death type was determined by a PE Annexin V Apoptosis Detection Kit with 7-AAD (BioLegend Inc.) according to the manufacturer's instructions. Briefly, the cells were suspended in 100 μL of Annexin V binding buffer, and then 5 μL of PE-conjugated Annexin V and 7-AAD was added to the samples. Following the incubation at room temperature for 15 min in the dark, the stained cells were examined using a FacsCanto Flow Cytometry (BD Bioscience, USA).

Ethidium Bromide/Acridine Orange Staining. Cells were seeded on the 6-well plate and treated with AG-08 or vehicle. After incubation of cells with 5 μg/mL acridine orange and 5 μg/mL ethidium bromide for 35 min at 37 °C, the cells were washed with PBS two times and then immediately analyzed by fluorescence microscopy (Olympus IX70, Japan).

Statistical Analysis. The statistical significance of differences between groups was assessed by two-tailed equal variance Student's *t* test using GraphPad Prism software.

RESULTS

Structural Characterization of AG-08. Astragenol (AG) was synthesized from cycloastragenol (CG) through acid hydrolysis. After the structure was established by comparing its NMR spectral data with those of previous reports[11,12] (Figures S8, S9), AG was treated with *p*-TsCl to obtain AG-08 (Figure 1). In the HR-ESI-MS of AG-08, a major ion peak was observed at m/z 649.36068 $[M + Na]^+$, indicating the molecular formula as $C_{37}H_{54}O_6S$ (Figure S1). Four protons (δ_H 7.8 and 7.32, each 2H) and additional methyl signals (δ_H 2.44, 3H) in the low-field region of the ^1H NMR spectrum implied tosyl addition to the AG (astragenol) skeleton. Also, ^1H, ^{13}C NMR, and HSQC spectra revealed a disubstituted double bond system (δ_C 126.2 and 127.3, each d; δ_H 5.60 and 5.61, each 1H). As the characteristic H-3 signal of AG shifted downfield to δ_H 4.31, the position of the tosyl group was readily deduced to be C-3(*O*). Moreover, the absence of oxymethine proton H-6 unambiguously located the aforementioned double bond at C-6(7) (Figures S2–S7). On the basis of this evidence, the structure of AG-08 was elucidated as 20(*R*),24(*S*)-epoxy-3(*O*)-*p*-tosyl-16β,25-dihydroxylanosta-6,9(11)-diene.

AG-08 Triggers Necrotic Cell Death Rather than Apoptosis. The antiproliferative effects of AG-08, CG, and AG were evaluated in various cancer and noncancer cell lines.

https://dx.doi.org/10.1021/acs.chemrestox.0c00339
Chem. Res. Toxicol. 2020, 33, 2880−2891

Unlike its starting molecules, AG-08 was found to display significant cytotoxicity (Table 1 and Table S2). Next, we

Table 1. AG-08 Exhibits Potent Inhibitory Activity against Several Cell Lines[a]

cell lines	IC_{50} (μM)
HCC1937	3.81 ± 0.272
DU145	3.46 ± 0.074
IMR-90	6.48 ± 0.166
H295R	4.41 ± 0.181
LNCaP	2.4 ± 0.075
C2C12	2.94 ± 0.112
Vero	4.45 ± 0.318
A549	2.3 0.035

[a]Data represented as mean ± standard error from the triplicate experiment (n = 3).

characterized AG-08-mediated cell death via multiple approaches. First, AG-08, but not staurosporine (an apoptotic inducer), treatment of the HCC1937 cell line resulted in dose-dependent lactate dehydrogenase (LDH) release, a well-known feature of the necrotic cell death due to the loss of membrane integrity (Figure 2A and Figure S10). Second, AG-08-treated cells were stained with EtBr in acridine orange (AO)/ethidium bromide (EtBr) staining assay, suggesting membrane integrity loss. Although staurosporine treatment also resulted in EtBr staining, the observation of bright green dots as a result of the condensed chromatin structure on AO staining strongly indicated apoptosis. On the other hand, similar to boiled water treatment, a known necrosis inducer, AG-08 treatment did not cause chromatin condensation and formation of green dots (Figure 2B). Third, AG-08-treated cells had necrotic nucleus morphology while staurosporine treatment caused typical apoptotic morphology in cells (Figure 2C). Fourth, labeling cells with Annexin V and 7-AAD revealed that AG-08 predominately caused an increase in 7-AAD positive cells (Figure 2D). Lastly, AG-08 treatment caused the formation of 50 kDa PARP-1 fragment associated with necrotic cell death, while 89 kDa cleaved-PARP-1 fragment, a hallmark for apoptosis, was detected by staurosporine treatment[13,14] (Figure 2E). Overall, the above-mentioned results demonstrate that AG-08 induces necrotic type cell death.

AG-08 Induces Lysosomal Membrane Permeabilization, Redistribution, and Tubulation. Since cathepsins, which are lysosomal proteases, are reported to be responsible for the formation of 50 kDa cleaved PARP-1 fragment,[13,15] we suspected that AG-08 might induce the lysosome membrane permeabilization and in turn trigger cathepsin release to the cytoplasm. In line with our suggestion, staining of HCC1937 and A549 cells with LysoTracker Red DND-99, a lysosomotropic dye specifically staining acidic lysosome and late endosome compartments, revealed that AG-08 treatment caused the loss of lysosomal acidity, implying damage in lysosome membrane integrity (Figure 3A and Figure S11A, B). Next, cathepsin B/L/S activity was measured in the cytoplasm after subcellular isolation of the cytoplasm and lysosome rich fractions to ascertain that AG-08 induces cathepsins leakage. As expected, AG-08 treatment leads to an increase in the cathepsin B/L/S activity in the cytoplasm (Figure 3B). Concomitantly, cathepsin inhibitor I (Cat I), which inhibits cathepsins B, L and S, protected cells from AG-08-mediated cell death (Figure 3C).

To investigate whether AG-08 required a healthy lysosome during the initiation of cell death, we pretreated cells with bafilomycin A1 (BafA1) to inhibit H^+-ATPase (V-ATPase) and thereby decrease the acidity of lysosomes. BafA1 efficiently reduced AG-08-inflicted cell death (Figure 3D). This result is evident that the activity of AG-08 requires healthy acidic lysosome, probably because acidity is necessary for the activation of cathepsins.

To further understand the effect of AG-08 on lysosome, the localization of LAMP-1 protein, the late endosome/lysosome (referred to as "lysosomes" for simplicity hereafter) marker was investigated. Although lysosomes were scattered throughout the cytoplasm in control cells, they were redistributed toward the perinuclear region by AG-08 treatment (Figure 3E). More interestingly, AG-08 triggered excessive tubulation of lysosomal membranes (Figure 3E).

As cholesterol has a role in the lysosomal positioning and tubulation,[16] we have also stained cellular cholesterol using filipin III. Cholesterol accumulation was observed in the perinuclear area within vesicular compartments resembling the tubules seen in lysosomes (Figure 3F). Thus, on further examination, cholesterol and lysosomes were costained proving the accumulation of cholesterol in lysosome (Figure S12C).

AG-08 Inhibits Autophagy. Given AG-08-driven lysosomal impairment, we were prompted to investigate its effect on autophagy, a lysosome-mediated intracellular degradation pathway. LC3 lipidation (LC3-II), a well-known autophagic marker,[17] was found to be increased upon AG-08 treatment in a dose-dependent manner in HCC1937 cells (Figure 4A), suggesting the accumulation of vacuoles due to autophagic flux inhibition. Since LC3-II accumulation may also occur during the autophagic activation, we have utilized additional markers and approaches to confirm the activity of AG-08 on autophagy. Interestingly, the levels of p62, another important autophagy marker, increased upon 4 μM AG-08 treatment, whereas 8 and 16 μM concentrations provided a significant reduction of p62 levels (Figure 4A). p62 usually accumulates during autophagic flux inhibition, and its decrease is an indicator of the autophagic activation. However, the cleavage of p62 by proteases, which in turn decreases the p62 protein levels, was also reported in some conditions where even autophagy was inhibited.[18] Likewise, we observed formation of 20 kDa fragments upon treatment of higher AG-08 concentrations accompanied with the decrease in full-length protein (Figure S12B). Moreover, similar p62 and LC3-I/II profiles were also detected in the A549 cell line, indicating autophagic flux inhibition was not limited to the HCC1937 cells (Figure S12A).

Based on the significant alteration at the protein level, we speculated that p62 protein might be accumulated due to the autophagic flux inhibition at the early stage, but subsequently it was cleaved by the activated proteases leading to the noteworthy decrease. Thus, we analyzed the levels of autophagy-related proteins in a time course experiment at 4 μM concentration. Indeed, p62 levels were augmented at 16 h, followed by a decrease at 36 h (Figure 4C). To clarify this intriguing observation, we wanted to eliminate the possibility of transcriptional alteration of p62 levels via AG-08 treatment and showed that AG-08 treatment did not cause any change in the mRNA level of p62 (Figure 4D), further suggesting that AG-08 inhibited autophagic flux. Similar to change seen on p62 protein levels, various Atg proteins were decreased by AG-08 treatment in a dose-dependent manner (Figure 4B and

https://dx.doi.org/10.1021/acs.chemrestox.0c00339
Chem. Res. Toxicol. 2020, 33, 2880−2891

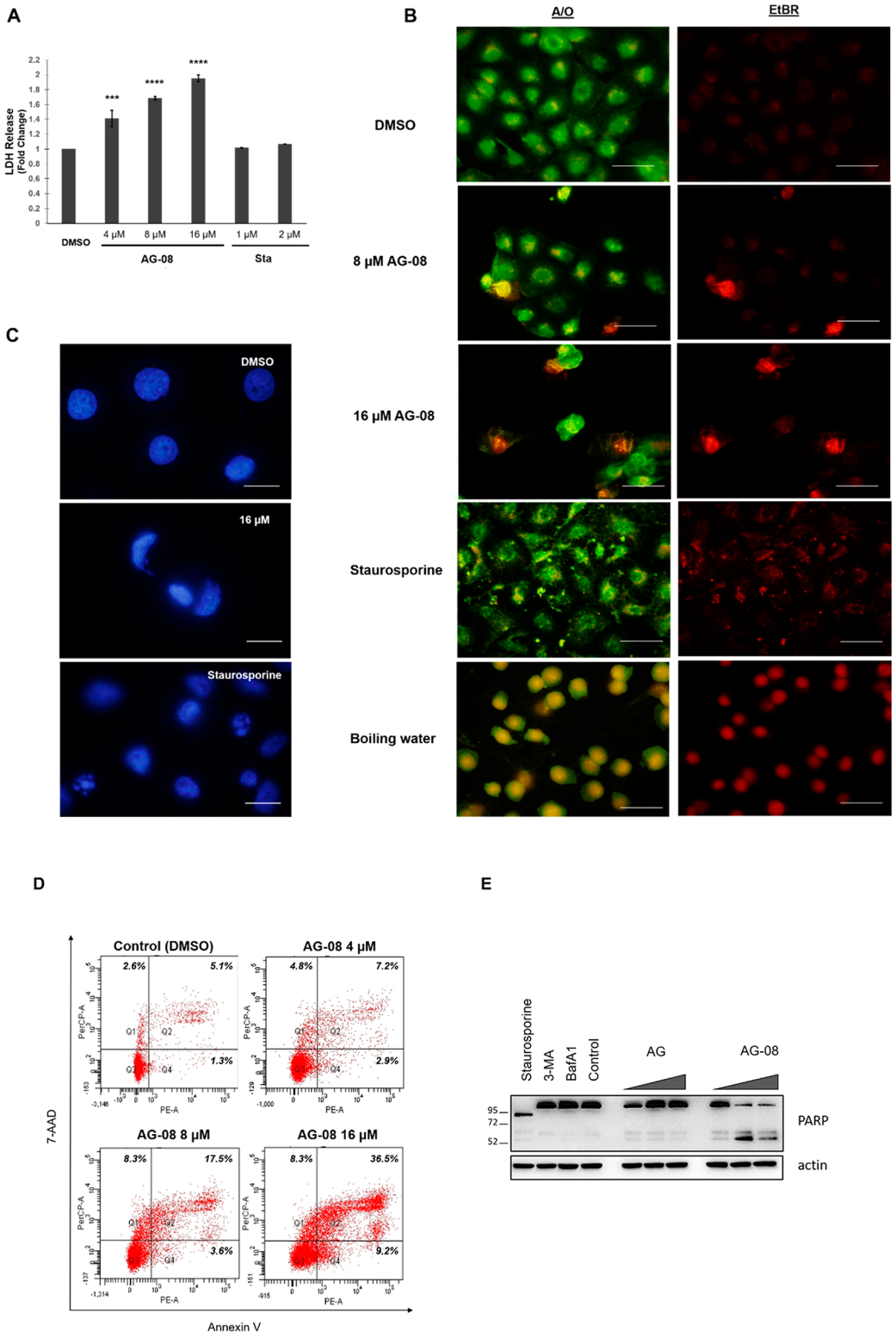

Figure 2. AG-08 induces necrotic cell death. (A) LDH release was determined after the treatment of cells with 4, 8, and 16 μM AG-08 or vehicle (DMSO) for 16 h. Staurosporine (Sta, 1 and 2 μM) was used to induce apoptosis as negative control for LDH release. The level of released LDH was calculated as the fold change relative to vehicle. The reported values correspond to mean values ± standard deviation (± s.d) of three experiments. ***$p < 0.001$, ****$p < 0.0001$. (B) After HCC1937 cells were treated with AG-08 (8 and 16 μM) for 16 h and 1 μM Sta for 8 h, cells were stained with ethidium bromide/acridine orange. Additionally, boiled water was added to cells for 2 min to induce necrosis (scale bar = 40 μm). (C) Following HCC1937 cells were treated with 16 μM AG-08 and 1 μM Sta for 16 h, and the nuclei of cells were stained with DAPI (scale bar = 25 μm). (D) HCC1937 cells stained by Annexin V/7-AAD and analyzed via flow cytometry after treatment with 4, 8, and 16 μM AG-08 or vehicle for 16 h. (E) After HCC1937 cells were treated with 7, 14, and 21 μM AG-08 or vehicle for 16 h, cleaved PARP-1 fragments were analyzed via immunoblotting (IB). Sta (1 μM) was used as an apoptotic inducer while 3-MA, bafilomycin A1 (Baf A1; 1 nM), and AG (10, 20, and 30 μM) were negative controls. The experiment was repeated three times independently, with one representative result shown.

https://dx.doi.org/10.1021/acs.chemrestox.0c00339
Chem. Res. Toxicol. 2020, 33, 2880−2891

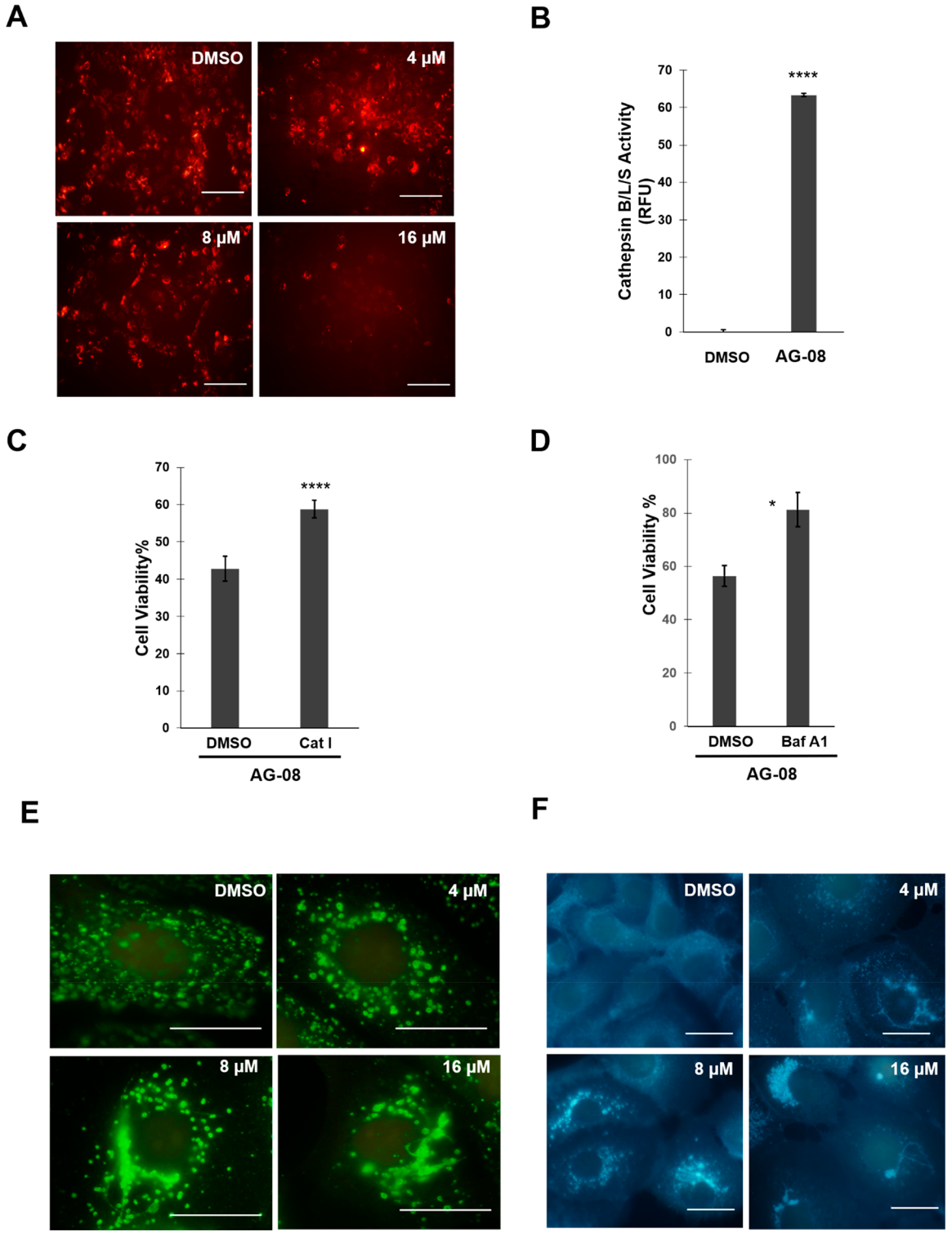

Figure 3. AG-08 intriguingly affects lysosome. (A) The lysosomal acidity of cells was determined by using LysoTracker Red DND-99. While red staining indicates acidic lysosome, nonstaining shows nonacidic lysosome (scale bar = 200 μm). (B) HCC1937 cells were treated with 16 μM AG-08 or vehicle for 16 h. Following obtaining the cytoplasmic fraction of cells, the cathepsin B/L/S activity was determined. (C) Following pretreatment with 50 μM cathepsin inhibitor I (CAT I) for 1 h, HCC1937 cells were treated with 8 μM AG-08 for 24 h. Then cell viability was calculated. (D) After pretreatment with 0.125 nm bafilomycin A1 (Baf A1) for 1 h, HCC1937 cells were treated with 8 μM AG-08 for 24 h. Error bars are the standard deviations (n = 3). p-Values were calculated with respect to vehicle-treated cells (*p < 0.05). (E) Lysosomal marker, LAMP1, was stained with specific antibody (scale bar = 25 μm). (F) Localization of cholesterol was investigated by using filipin III staining (scale bar = 25 μm).

Figure S12C), without any change in their mRNA levels (Figure S12E, F). In line with autophagic flux, Atg proteins levels were also decreased in A549 cells (Figure S12D). Interestingly, even though 8 and 16 μM AG-08 decreased the

https://dx.doi.org/10.1021/acs.chemrestox.0c00339
Chem. Res. Toxicol. 2020, 33, 2880−2891

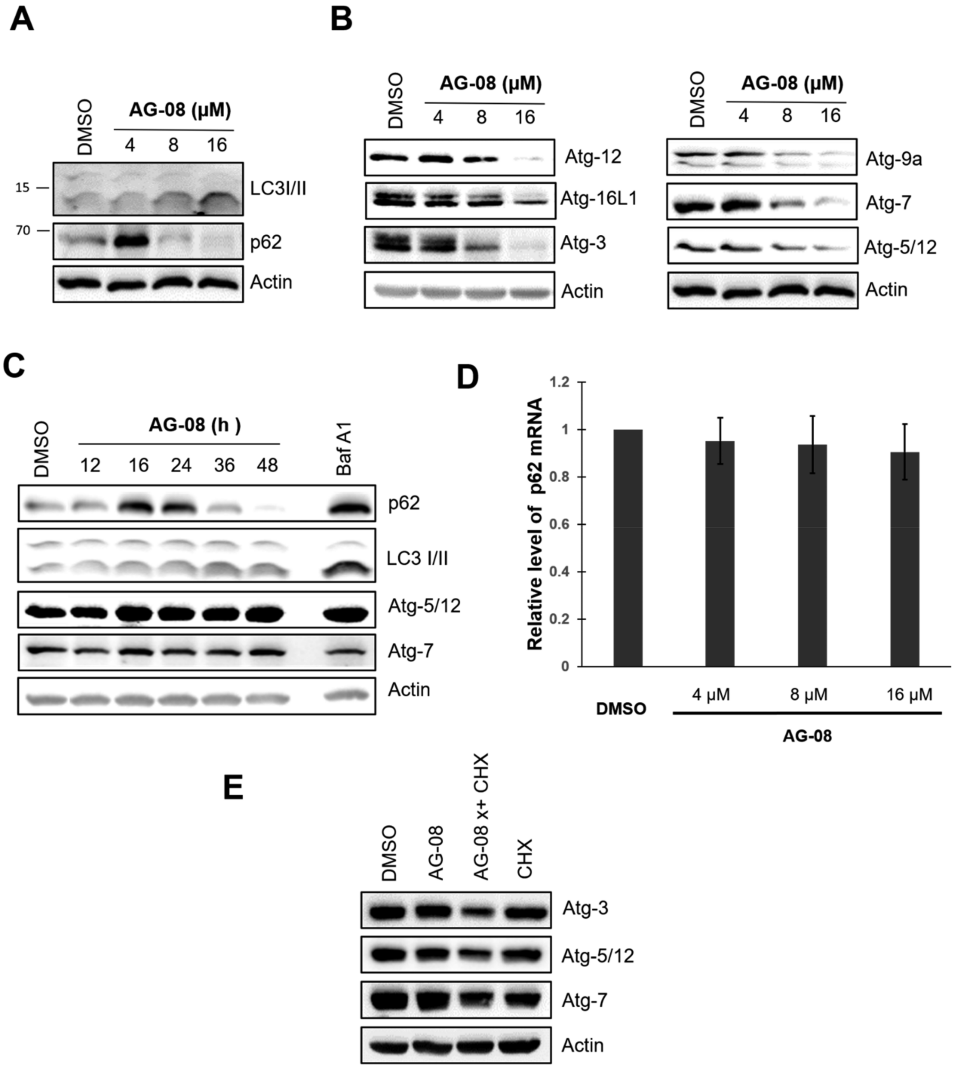

Figure 4. AG-08 inhibits autophagy. (A–B) HCC1937 cells were treated with 4, 8, and 16 μM AG-08 or vehicle for 16 h. (A) Conversion of LC3-I to LC3-II and p62 level was determined via IB. (B) The levels of Atg-5/12, Atg-7, Atg-3, and Atg-9a were detected by IB using antibodies against them. (C) AG-08 (4 μM) was used to determined time-dependent change in LC3-I/LC3-II, p62, and Atgs levels. (D) After HCC1937 cells were treated with 4, 8, and 16 μM AG-08 or vehicle for 16 h, the mRNA level of the p62 was examined by q-RTPCR. Error bars represent the standard error. (E) After pretreatment with 0.5 μM cycloheximide (CHX) for 1 h, HCC1937 cells were treated with 8 μM AG-08 for 16 h. Then, levels of Atg-5/12, Atg-7, and Atg-3 were determined via IB. The experiments were repeated three times independently, with one representative result shown.

Atg protein levels at 16 h (Figure 4B), no changes in their levels were detected with 4 μM concentration with prolonged exposure up to 48 h (Figure 4C). Next, we have cotreated cells with a protein synthesis inhibitor (cycloheximide: CHX) to observe any possible slight alterations in Atg protein levels. Significant decreases in Atg-3, -5, and -7 protein levels were observed with the CHX and AG-08 cotreatment, compared to those with CHX alone (Figure 4E), suggesting that the 4 μM concentration of AG-08 indeed decreases Atg protein levels.

Moreover, we investigated effect of early stage autophagy inhibition and induction of autophagic vacuole formation on AG-08-mediated cell death by using 3-MA and rapamycin, respectively. Results showed that both 3-MA and rapamycin were not able to rescue cells from the cytotoxicity of AG-08 (Figure S12G–H).

Calpains Are One of the Main Players in AG-08-Generated Cell Death. Based on several reports indicating that calpains and caspases are responsible proteases for the cleavage of Atgs, we next investigated the effect of AG-08 on the activity of calpains, calcium-dependent proteases.[19−22] AG-08 was found to significantly induce the calpain activity in a dose-dependent manner (Figure 5A and Figure S13B). Moreover, the inhibition of calpains by calpeptin attenuated the cell death, showing that calpains played an important role in AG-08-mediated cell death (Figure 5B).

AG-08-Mediated Necrosis Is Caspase Dependent. After calpain activation was observed, the effect of AG-08 on the activity of caspases was also investigated. First, we observed that AG-08 induced the activation of caspase-3 and -7, the effector proteins (Figure 6A). Also, among initiator caspases, caspase-8 but not caspase-9 was activated by AG-08 (Figure 6B). Subsequently, both Z-VAD-fmk (general caspase inhibitor) and Z-IETD-fmk (caspase 8 inhibitor) lessened the AG-08-mediated cell death while general caspase inhibitor was found to be more efficient (Figure 6C). Thus, AG-08

https://dx.doi.org/10.1021/acs.chemrestox.0c00339
Chem. Res. Toxicol. 2020, 33, 2880−2891

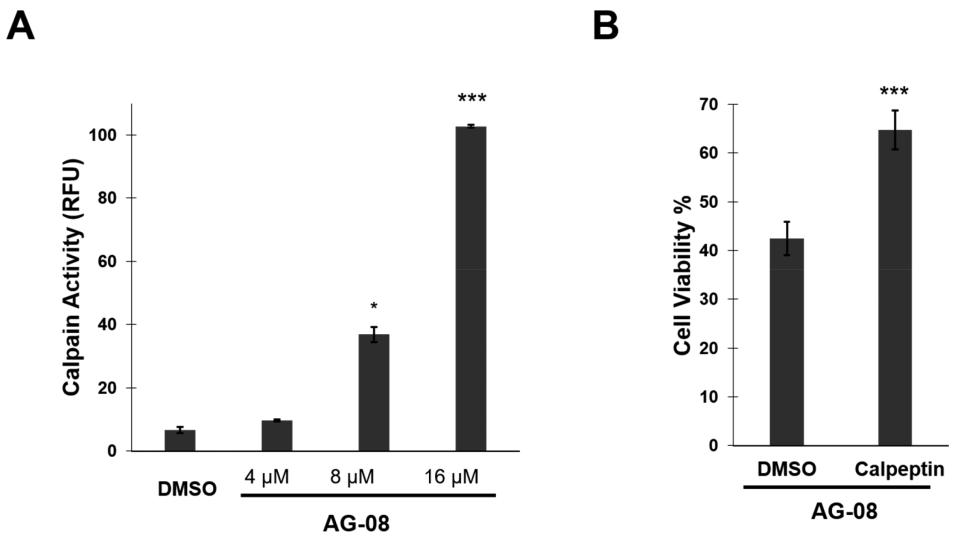

Figure 5. Calpains are one of the main players in cell death via AG-08. (A) HCC1937 cells were treated with 4, 8, and 16 μM AG-08 or vehicle for 16 h, and calpain activity was determined. p-Values were calculated with respect to vehicle-treated cells. (B) HCC1937 cells were treated with 30 μM calpeptin for 1 h and then treated with 8 μM AG-08. Cell viability was determined after 24 h. (*p-value <0.05, ***p-value <0.001).

induces a noncanonical necrotic cell death, which is caspase dependent.

AG-08 Induces Proteasome Activity. Since autophagy and the ubiquitin−proteasome system are the main pathways of the cellular protein degradation, we next investigated the effect of AG-08 on the activity of proteasome. First, AG-08 treatment decreased the K48-linked polyubiquitin levels, which might indicate enhanced proteasomal activity (Figure 7A). The use of the fluorogenic substrate (Suc-Leu-Leu-Val-Tyr AMC) to measure the chymotrypsin-like activity of 20S proteasome further revealed that AG-08 treatment increased the proteasomal activity (Figure 7B). Interestingly, when cell lysate was treated directly with AG-08, no significant change was observed suggesting that AG-08 might indirectly induce the proteasomal activity (Figure 7C). To investigate whether the increased activity of proteasome by AG-08 had any initiator role on the observed cell death, cells were pretreated with bortezomib, a commercial proteasome inhibitor compound. However, no significant effect of proteasome inhibition on cell death was observed (Figure 7D) suggesting that proteasome was activated as a secondary stress response without a direct role in AG-08-induced cell death.

DISCUSSION

The semisynthesis approach is utilized to enhance the antitumor activity of various saponins. The work described here reveals a new cytotoxic sapogenin derivative, viz., AG-08, prepared from a noncytotoxic parent compound (CG). Our data have clearly shown that AG-08 induces noncanonical cell death with necrotic features. After the discovery of regulated necrosis, the induction of necrotic cell death has attracted huge attention, and numerous studies state that necrotic cell inducers possess high potential for cancer treatment. Concomitantly, some FDA-approved chemotherapeutics have been reported to induce necrotic cell death, further emphasizing the potential of targeting necrosis for anticancer therapy.[8,9,23] Additionally, the necrotic cell death has been also stated for intratumoral therapy since it is able to activate an antitumor immune response. Strikingly, ongoing clinical studies with two necrotic compounds (PV-10 and EBC-46) for intratumoral injection prove the potential of the necrotic cell death inducers.[24−26]

Since the resistance to apoptotic chemotherapeutics is one of the main obstacles to successful cancer therapy, nonapoptotic cell death such as regulated necrosis becomes a potent strategy to overcome drug resistance. For instance, necroptosis is put forward as a novel therapeutic strategy for overcoming common apoptosis resistance in leukemia,[27,28] and ferroptosis was reported as a novel perspective to cope with cisplatin resistance in nonsmall cell lung cancer.[29] Moreover, the use of necrotic cell death initiators in combination with current chemotherapy agents is a logical alternative for drug development studies because simultaneous activation of different pathways with multiple drugs/drug candidates may cope with failure of the treatment due to intraheterogeneity.[30,31] Unlike traditional cancer drugs, the noncanonical necrotic cell death mechanism of AG-08 makes it a highly potential antitumor drug candidate. In addition, the impairment of autophagy and lysosome, which are known to play major roles in the drug resistance, strengthens this potential.

The cellular proteases are effective players of the cell death as their functions are irreversible. We have shown that AG-08 causes an increase in the activity of cathepsins in cytoplasm accompanied by the loss of the acidic nature of lysosomes indicating the release of the lysosomal content to the cytoplasm. Besides cathepsins, two other important protease families, viz., calpains and caspases, are also activated by AG-08 treatment. Moreover, inhibition of these proteases attenuated AG-08-mediated cell death; thus, AG-08 is proposed to be an effective inducer of general proteolysis.

The activation of caspase-3, -7, and -8 is an interesting feature of AG-08-mediated necrotic cell death since these caspases are well-known apoptotic effectors. However, there are some recent studies emphasizing that caspase activation does not always reflect apoptosis or vice versa. For instance, caspase-dependent neuronal necrosis was reported via hypoxia in the presence of blockers of excitotoxicity[32] or via TRAIL under acidic extracellular conditions.[33] In line with that, a limited number of compounds such as cisplatin and chelerythrine were reported to induce necrosis accompanied

https://dx.doi.org/10.1021/acs.chemrestox.0c00339
Chem. Res. Toxicol. 2020, 33, 2880−2891

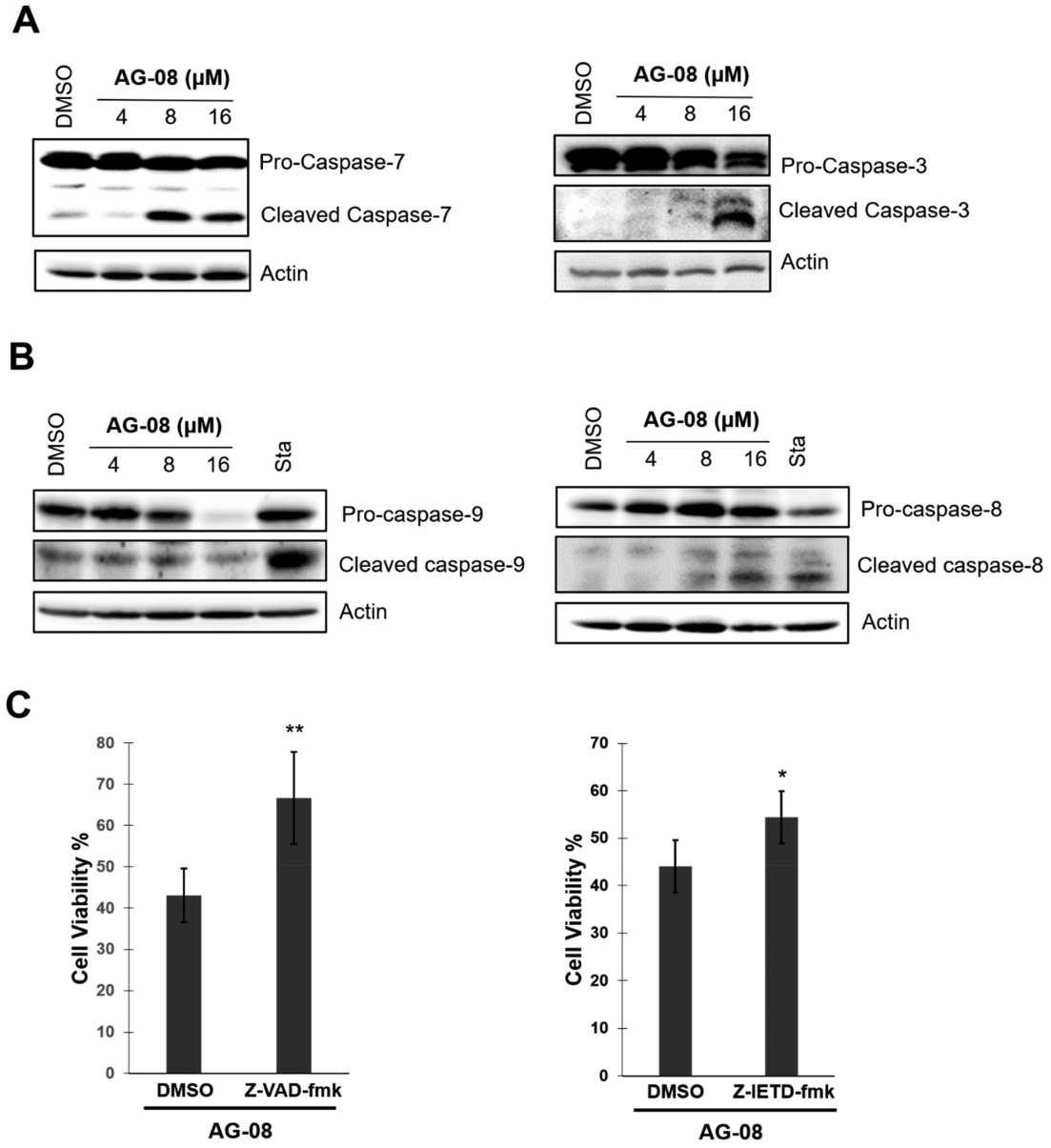

Figure 6. AG-08 activates caspases. (A–B) HCC1937 cells were treated with 4, 8, and 16 μM AG-08 or vehicle for 16 h, and expression levels of full length and cleaved caspase-3, -7, -8, and -9 were determined via IB. Representative data from three independent experiments are shown. (C) After pretreatment with 70 μM Z-VAD-fmk or 30 μM Z-IETD-fmk for 1 h, HCC1937 cells were treated with 8 μM AG-08 for 24 h. Then cell viability was determined via WST-1. Error bars are the standard deviations from three independent experiments (*p-value <0.05, **p-value <0.005).

by caspases activation.[34−37] Collectively, in addition to identifying AG-08 as an inducer of caspase-dependent necrotic cell death, our study once again has demonstrated that there are no precisely characterized boundaries between cell death types.

Lysosomes are mainly affected by AG-08. Lysosomes were redistributed toward the perinuclear region in AG-08-treated cells. Although the accumulation of lysosomes in the perinuclear area is usually reported in the case of the excessive activation of autophagy, our results strongly suggest that autophagy is inhibited by AG-08 treatment. Other factors that cause the perinuclear clustering of lysosomes are stated as TRPML1 (Ca^{2+} channel in the lysosome) inhibition or cholesterol accumulation in lysosome as seen in various lysosomal disorders.[16,38] Since TRPML1 inhibition has been shown to block lysosome tubulation, the activity of AG-08 should be independent of TRPML1 inhibition.[16] Therefore, we suggest that lysosomal redistribution mediated by AG-08 might be a result of the cholesterol accumulation.

Our results interestingly show that AG-08 is also an inducer of the lysosomal tubulation. Although the lysosomal tubulation is a poorly characterized biological process, there are some reports suggesting that it provides replenishment of the functional lysosomes. This may occur for the reformation of lysosomes during excessive use as in prolonged starvation or antigen presentation[16,39] or when the vesicle budding from lysosomal membrane is inhibited.[40] We speculate that AG-08-mediated lysosomal tubulation may be the result of inhibition of vesicle budding since lysosomal overactivation is not likely since AG-08 induces the lysosomal impairment.

Additionally, autophagic flux inhibition, which is one of the other consequences of lysosomal disorder, is also demon-

https://dx.doi.org/10.1021/acs.chemrestox.0c00339
Chem. Res. Toxicol. 2020, 33, 2880−2891

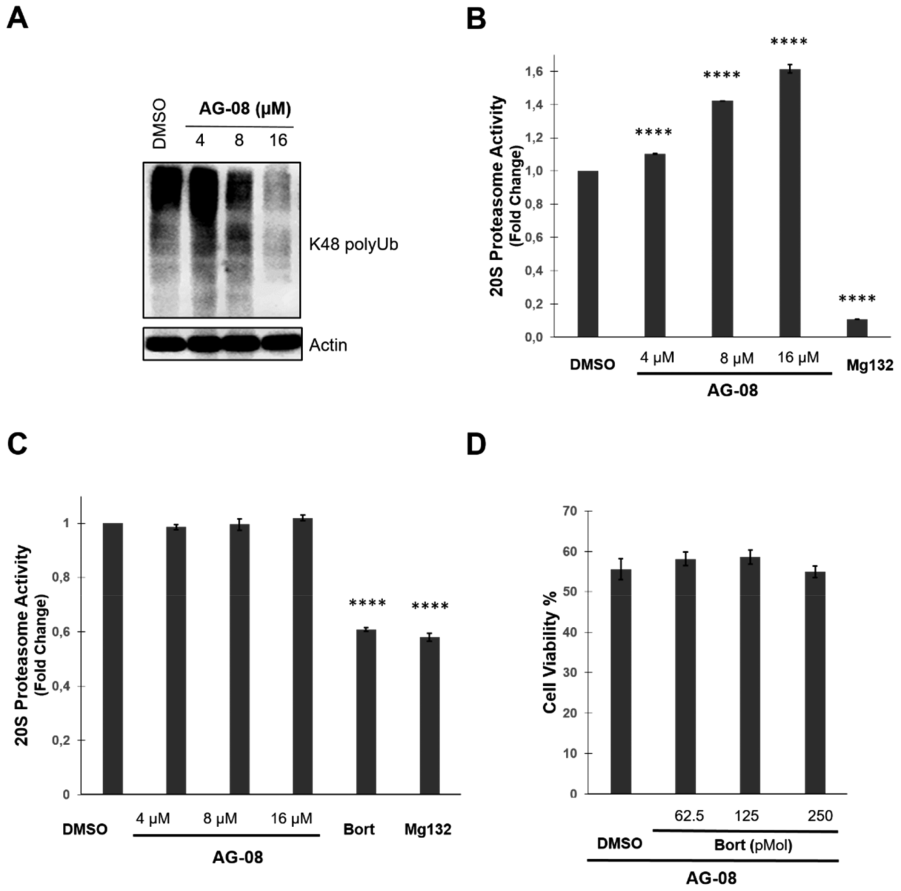

Figure 7. AG-08 indirectly activates proteasome. (A–B) HCC1937 cells were treated with 4, 8, and 16 μM AG-08 or vehicle for 16 h. (A) The level of K48-linked ubiquitinated proteins was determined by IB. (B) Proteasomal activity was determined via Suc-Leu-Leu-Val-Tyr AMC. Mg132 (1 μM) was used as a proteasome inhibitor. Reported values were normalized to cells treated with vehicle. *p*-Values were calculated with respect to vehicle-treated cells (****$p < 0.0001$). (C) The proteasome rich lysate of untreated cells was incubated with AG-08, vehicle, or proteasome inhibitors (100 pmol bortezomib (Bort) and 10 μM Mg132), and then proteasomal activity was determined and reported as in Figure 6B (****$p < 0.0001$). (D) Following pretreatment with Bort, HCC1937 cells were treated with 8 μM AG-08 for 24 h. Then cell viability was determined (****$p < 0.0001$).

strated via AG-08 treatment. Interestingly, the dramatic decrease in the levels of several Atgs suggests the inhibition of autophagic vacuole formation since Atgs are required for this process. In line with Atgs, the levels of p62 was increased upon 4 μM AG-08 treatment, whereas 8 and 16 μM concentrations induced reduction of p62 levels probably due to protease activation. Therefore, it is sound to suggest that AG-08 inhibits autophagy at two stages; first, autophagic flux is inhibited, and vacuoles are accumulated. Then the formation of autophagic vacuoles is abolished via the cleavage of Atg proteins.

Consequently, AG-08 has the potential to become an interesting lead compound for anticancer drug research because of its capability to activate different pathways leading to cell death. Further studies are warranted to establish structure–activity relationships via synthesis of AG-08 derivatives and to clarify the thorough mechanism of AG-08.

■ ASSOCIATED CONTENT

Supporting Information

The Supporting Information is available free of charge at https://pubs.acs.org/doi/10.1021/acs.chemrestox.0c00339.

^{13}C and ^{1}H NMR data of AG-08; HR-ESI-MS spectrum of AG-08; NMR spectra of AG-08 and AG; time-dependent LDH releasing with AG-08; additional data indicating that AG-08 induces lysosomal impairment; additional data showing that AG-08 inhibits autophagy; calpain and caspase activation via AG-08 in the A459 cell line; Western blot densitometric analysis of Figure 4; cytotoxicity of AG and CG; q-RT-PCR primer list (PDF).

■ AUTHOR INFORMATION

Corresponding Authors

Erdal Bedir – *Department of Bioengineering, Izmir Institute of Technology, 35430 Urla, İzmir, Turkey*; orcid.org/0000-0003-1262-063X; Email: erdalbedir@iyte.edu.tr

Petek Ballar Kirmizibayrak – *Department of Biochemistry, Faculty of Pharmacy, Ege University, 35100 Bornova, İzmir, Turkey*; Email: petek.ballar@ege.edu.tr

Authors

Göklem Üner – *Department of Bioengineering, Izmir Institute of Technology, 35430 Urla, İzmir, Turkey*

Özgür Tağ – *Bionorm Natural Products Production & Marketing Corporation, ITOB, 35477 Menderes, İzmir, Turkey*

Yalçın Erzurumlu – *Department of Biochemistry, Faculty of Pharmacy, Ege University, 35100 Bornova, İzmir, Turkey*

https://dx.doi.org/10.1021/acs.chemrestox.0c00339
Chem. Res. Toxicol. 2020, 33, 2880–2891

Complete contact information is available at:
https://pubs.acs.org/10.1021/acs.chemrestox.0c00339

Author Contributions

P.B.K and E.B. formed the hypothesis and designed the study. Ö.T. and G.Ü. purified the starting compounds and performed synthesis studies. G.Ü. participated in the experimental design and conducted most of the experiments and collected data. Y.E. performed some preliminary experiments. P.B.K, E.B, and G.Ü. analyzed the results and contributed to the manuscript preparation. All authors read and approved the manuscript.

Funding

This project was supported by The Scientific and Technological Research Council of Turkey (TUBITAK, Project No: 118S709) as a continuation of a prior project (TUBITAK, Project No: 109S345).

Notes

The authors declare no competing financial interest.

■ ACKNOWLEDGMENTS

We are very grateful to Bionorm Natural Products for donating cycloastragenol, and special thanks to the Pharmaceutical Sciences Research Centre (FABAL, Ege University, Faculty of Pharmacy) and Biotechnology and Bioengineering Application and Research Centre (BİYOMER, İzmir Institute of Technology) for equipment support.

■ REFERENCES

(1) Sparg, S., Light, M., and Van Staden, J. (2004) *J. Ethnopharmacol. 94*, 219−243.
(2) Honda, T., Rounds, B. V., Bore, L., Finlay, H. J., Favaloro, F. G., Suh, N., Wang, Y., Sporn, M. B., and Gribble, G. W. (2000) Synthetic oleanane and ursane triterpenoids with modified rings A and C: a series of highly active inhibitors of nitric oxide production in mouse macrophages. *J. Med. Chem. 43*, 4233−4246.
(3) Zahreddine, H., and Borden, K. (2013) Mechanisms and insights into drug resistance in cancer. *Front. Pharmacol. 4*, 28.
(4) Ricci, M. S., and Zong, W. X. (2006) *Oncologist 11*, 342.
(5) Chen, L., Zeng, Y., and Zhou, S. F. (2018) Role of Apoptosis in Cancer Resistance to Chemotherapy. *Current Understanding of Apoptosis-Programmed Cell Death*.
(6) Gong, Y., Fan, Z., Luo, G., Yang, C., Huang, Q., Fan, K., Cheng, H., Jin, K., Ni, Q., and Yu, X. J. M. C. (2019) Role of necroptosis in cancer biology and therapy. *Mol. Cancer 18*, 1−17.
(7) Cho, Y. S., and Park, S. Y. J. B. (2014) Harnessing of Programmed Necrosis for Fighting against Cancers. *Biomol. Ther. 22*, 167.
(8) Okada, M., Adachi, S., Imai, T., Watanabe, K.-İ., Toyokuni, S.-Y., Ueno, M., Zervos, A. S., Kroemer, G., and Nakahata, T. (2004) A novel mechanism for imatinib mesylate-induced cell death of BCR-ABL-positive human leukemic cells: caspase-independent, necrosis-like programmed cell death mediated by serine protease activity. *Blood 103*, 2299−2307.
(9) Wu, P., Zhu, X., Jin, W., Hao, S., Liu, Q., and Zhang, L. (2015) Oxaliplatin triggers necrosis as well as apoptosis in gastric cancer SGC-7901 cells. *Biochem. Biophys. Res. Commun. 460*, 183−190.
(10) Louandre, C., Ezzoukhry, Z., Godin, C., Barbare, J. C., Mazière, J. C., Chauffert, B., and Galmiche, A. (2013) Iron-dependent cell death of hepatocellular carcinoma cells exposed to sorafenib. *Int. J. Cancer 133*, 1732−1742.
(11) Kitagawa, I., Wang, H., Takagi, A., Fuchida, M., Miura, I., and Yoshikawa, M. (1983) Saponin and sapogenol. XXXIV. chemical constituents of astragali radix, the root of Astragalus membranaceus Bunge. (1). Cycloastragenol, the 9, 19-cycloanostane-type aglycone of astragalosides, and the artifact aglycone astragenol. *Chem. Pharm. Bull. 31*, 689−697.
(12) Feng, L. M., Lin, X. H., Huang, F. X., Cao, J., Qiao, X., Guo, D. A., and Ye, M. (2014) Smith degradation, an efficient method for the preparation of cycloastragenol from astragaloside IV. *Fitoterapia 95*, 42−50.
(13) Chaitanya, G. V., Alexander, J. S., and Babu, P. P. (2010) PARP-1 cleavage fragments: signatures of cell-death proteases in neurodegeneration. *Cell Commun. Signaling 8*, 31.
(14) Casiano, C. A., Ochs, R. L., and Tan, E. M. (1998) Distinct cleavage products of nuclear proteins in apoptosis and necrosis revealed by autoantibody probes. *Cell Death Differ. 5*, 183−190.
(15) Gobeil, S., Boucher, C., Nadeau, D., and Poirier, G. (2001) Characterization of the necrotic cleavage of poly(ADP-ribose) polymerase (PARP-1): implication of lysosomal proteases. *Cell Death Differ. 8*, 588−594.
(16) Li, X., Rydzewski, N., Hider, A., Zhang, X., Yang, J., Wang, W., Gao, Q., Cheng, X., and Xu, H. (2016) A molecular mechanism to regulate lysosome motility for lysosome positioning and tubulation. *Nat. Cell Biol. 18*, 404−417.
(17) Tanida, I., Ueno, T., and Kominami, E. (2004) LC3 conjugation system in mammalian autophagy. *Int. J. Biochem. Cell Biol. 36*, 2503−2518.
(18) Klionsky, D. J., Abdelmohsen, K., Abe, A., Abedin, M. J., Abeliovich, H., Acevedo Arozena, A., Adachi, H., and Adams, C. M. (2016) Guidelines for the use and interpretation of assays for monitoring autophagy. *Autophagy 12*, 1−222.
(19) Norman, J. M., Cohen, G. M., and Bampton, E. T. W. (2010) The in vitro cleavage of the hAtg proteins by cell death proteases. *Autophagy 6*, 1042−1056.
(20) Zhu, Y., Zhao, L., Liu, L., Gao, P., Tian, W., Wang, X., Jin, H., Xu, H., and Chen, Q. (2010) Beclin 1 cleavage by caspase-3 inactivates autophagy and promotes apoptosis. *Protein Cell 1*, 468−477.
(21) Yousefi, S., Perozzo, R., Schmid, I., Ziemiecki, A., Schaffner, T., Scapozza, L., Brunner, T., and Simon, H. U. (2006) Calpain-mediated cleavage of Atg5 switches autophagy to apoptosis. *Nat. Cell Biol. 8*, 1124−1132.
(22) Cho, D.-H., Jo, Y. K., Hwang, J. J., Lee, Y. M., Roh, S. A., and Kim, J. C. (2009) Caspase-mediated cleavage of ATG6/Beclin-1 links apoptosis to autophagy in HeLa cells. *Cancer Lett. 274*, 95−100.
(23) Lachaier, E., Louandre, C., Godin, C., Saidak, Z., Baert, M., Diouf, M., Chauffert, B., and Galmiche, A. (2014) Sorafenib induces ferroptosis in human cancer cell lines originating from different solid tumors. *Anticancer Res. 34*, 6417−6422.
(24) Thompson, J. F., Hersey, P., and Wachter, E. (2008) Chemoablation of metastatic melanoma using intralesional Rose Bengal. *Melanoma Res. 18*, 405−411.
(25) Toomey, P., Kodumudi, K., Weber, A., Kuhn, L., Moore, E., Sarnaik, A. A., and Pilon-Thomas, S. (2013) Intralesional injection of rose bengal induces a systemic tumor-specific immune response in murine models of melanoma and breast cancer. *PLoS One 8*, No. e68561.
(26) Boyle, G. M., D'Souza, M. M., Pierce, C. J., Adams, R. A., Cantor, A. S., Johns, J. P., Maslovskaya, L., Gordon, V. A., Reddell, P. W., and Parsons, P. G. (2014) Intra-lesional injection of the novel PKC activator EBC-46 rapidly ablates tumors in mouse models. *PLoS One 9*, No. e108887.
(27) Huang, X., Xiao, F., Li, Y., Qian, W., Ding, W., and Ye, X. (2018) Bypassing drug resistance by triggering necroptosis: recent advances in mechanisms and its therapeutic exploitation in leukemia. *J. Exp. Clin. Cancer Res. 37*, 310.
(28) Huang, X., Jin, J., Qian, W., and Ye, X. (2019) *Shikonin Overcomes Drug Resistance and Induces Necroptosis By Regulating the Mir-92a-1-5p/Mlkl Axis in Chronic Myeloid Leukemia Cells*; American Society of Hematology, Washington, DC.
(29) Li, Y., Yan, H., Xu, X., Liu, H., Wu, C., and Zhao, L. (2019) Erastin/sorafenib induces cisplatin-resistant non-small cell lung cancer cell ferroptosis through inhibition of the Nrf2/xCT pathway. *Oncol. Lett. 19*, 323−333.

(30) Dagogo-Jack, I., and Shaw, A. T. (2018) Tumour heterogeneity and resistance to cancer therapies. *Nat. Rev. Clin. Oncol. 15*, 81.
(31) Mokhtari, R. B., Homayouni, T. S., Baluch, N., Morgatskaya, E., Kumar, S., Das, B., and Yeger, H. (2017) Combination therapy in combating cancer. *Oncotarget 8*, 38022.
(32) Niquet, J., Seo, D. W., Allen, S. G., and Wasterlain, C. G. (2006) Hypoxia in presence of blockers of excitotoxicity induces a caspase-dependent neuronal necrosis. *Neuroscience 141*, 77−86.
(33) Meurette, O., Rebillard, A., Huc, L., Le Moigne, G., Merino, D., Micheau, O., Lagadic-Gossmann, D., and Dimanche-Boitrel, M. T. (2007) TRAIL induces receptor-interacting protein 1-dependent and caspase-dependent necrosis-like cell death under acidic extracellular conditions. *Cancer Res. 67*, 218−226.
(34) Gonzalez, P., Mader, I., Tchoghandjian, A., Enzenmuller, S., Cristofanon, S., Basit, F., Debatin, K. M., and Fulda, S. (2012) Impairment of lysosomal integrity by B10, a glycosylated derivative of betulinic acid, leads to lysosomal cell death and converts autophagy into a detrimental process. *Cell Death Differ. 19*, 1337−1346.
(35) Deng, J.-Y., Chen, S.-J., Jow, G.-M., Hsueh, C.-W., and Jeng, C.-J. (2009) Dehydroeburicoic acid induces calcium-and calpain-dependent necrosis in human U87MG glioblastomas. *Chem. Res. Toxicol. 22*, 1817−1826.
(36) Dursun, B., He, Z., Somerset, H., Oh, D. J., Faubel, S., and Edelstein, C. L. (2006) Caspases and calpain are independent mediators of cisplatin-induced endothelial cell necrosis. *Am. J. Physiol Renal Physiol 291*, F578−587.
(37) Garcia-Belinchon, M., Sanchez-Osuna, M., Martinez-Escardo, L., Granados-Colomina, C., Pascual-Guiral, S., Iglesias-Guimarais, V., Casanelles, E., Ribas, J., and Yuste, V. J. (2015) An early and robust activation of caspases heads cells for a regulated form of necrotic-like cell death. *J. Biol. Chem. 290*, 20841−20855.
(38) Marques, A. R. A., and Saftig, P. (2019) Lysosomal storage disorders - challenges, concepts and avenues for therapy: beyond rare diseases. *J. Cell Sci. 132*, jcs221739.
(39) Saffi, G. T., and Botelho, R. J. (2019) Lysosome fission: Planning for an exit. *Trends Cell Biol. 29*, 635−646.
(40) Sridhar, S., Patel, B., Aphkhazava, D., Macian, F., Santambrogio, L., Shields, D., and Cuervo, A. M. (2012) The lipid kinase PI4KIIIbeta preserves lysosomal identity. *EMBO J. 32*, 324−339.

https://dx.doi.org/10.1021/acs.chemrestox.0c00339
Chem. Res. Toxicol. 2020, 33, 2880−2891